On the effect of compressibility on the impact of a falling jet

Paul Christodoulides[1], Frédéric Dias[2,3], Jean-Michel Ghidaglia[3], Marc Kjerland[3]
[1]Cyprus University of Technology, Cyprus
[2]University College Dublin, Ireland
[3]Centre de Mathématiques et de Leurs Applications, Ecole Normale Supérieure de Cachan and CNRS, France

ABSTRACT

At the first World Sloshing Dynamics Symposium that took place during the Nineteenth (2009) International Offshore and Polar Engineering (ISOPE) Conference in Osaka, Japan, it was made clear that simplified academic problems have an important role to play in the understanding of liquid impacts.
The problem of the impact of a mass of liquid on a solid structure is considered. First the steady two-dimensional and irrotational flow of an inviscid and incompressible fluid falling from a vertical pipe, hitting a horizontal plate and flowing sideways, is considered. A parametric study shows that the flow can either leave the pipe tangentially or detach from the edge of the pipe. Two dimensionless numbers come into play: the Froude number and the aspect ratio between the falling altitude and the pipe width. When the flow leaves tangentially, it can either be diverted immediately by the plate or experience squeezing before being diverted. The profile of the pressure exerted on the plate is computed and discussed. Then the same problem is revisited with the inclusion of compressibility effects, both for the falling liquid and for the gas surrounding it. An additional dimensionless number comes into play, namely the Mach number.
Finally, a discussion on the differences between the incompressible and compressible cases is provided.

KEY WORDS: Jet; liquid impact; dimensionless number; free-surface flow

INTRODUCTION

The problem of a liquid jet impacting on a wall is a classical one, with very practical applications, in particular in sloshing. Indeed the impact of a fluid on a solid boundary often occurs as a mass of liquid pushing the gas around it and hitting the structure ahead. It is a complex fluid mechanics problem as suggested by some of its features, such as: the nonlinearity of its free surface; the possible presence and importance of the compressibility effects, when gas is trapped by the liquid; the role of the elasticity of its structure. A description of all phenomena which can take place when a liquid jet hits a structure was provided by Braeunig et al. (2009) at ISOPE 2009. It was emphasized that simplified or academic impact conditions can be quite useful in understanding various phenomena.
The simpler problem of an infinite falling jet has already led to several papers, at least in the context of incompressible flows. The main motivation was the study of a long bubble rising through an infinite plane vertical tube of liquid. This problem can be actually viewed – if one uses a co-ordinate system attached to the bubble – as a liquid falling around a bubble, instead of the bubble rising in the liquid. The problem of an incompressible falling jet impacting on a horizontal plate was solved recently by Christodoulides and Dias (2010). The main results of that paper will be reviewed. Then we provide a better understanding of the compressible flow impacting on a solid plate. Since the geometry is exactly the same for the incompressible and the compressible cases, the geometric description is provided only once.

A stream of liquid flows down and out of the bottom of a long two-dimensional vertically-sided pipe of half-width W. The downwardly directed flow meets a horizontal plate of infinite extent set at a distance H below the bottom end of the pipe. The flow splits into two jets on each side of the pipe following a path along the horizontal plate. The general solution depends on the ratio H/W, on the dimensionless Froude number

$$F = \frac{U}{\sqrt{gW}}, \tag{1}$$

where g is the acceleration due to gravity and U the velocity of the fluid far inside the pipe, and on the Mach number

$$M = \frac{U}{c}, \tag{2}$$

where c is the speed of sound in the liquid. The incompressible case corresponds to the limit $M = 0$. A major difference between the incompressible and compressible cases is that the gas motion is modeled as well in the compressible case. Therefore there is an additional dimensionless number, which is the density ratio between the

gas density and the liquid density.

The results obtained by Christodoulides and Dias (2010) for the incompressible case ($M = 0$) are summarized in Figure 1. There are three regions in the (F, H/W) plane. These regions are divided by two curves, which were found numerically. One goes from region I to region III by increasing the velocity U at fixed H. In region I, the jet emerges from the pipe with a stagnation point. In region II, the jet emerges from the pipe without a stagnation point but experiences squeezing before being deflected by the horizontal plate. In region III, the jet emerges from the pipe without a stagnation point and is immediately deflected.

The theory of functions of complex variables and conformal mappings was used to obtain a new formulation of the problem particularly well-suited for discretization. A collocation method was then used to find the solution.

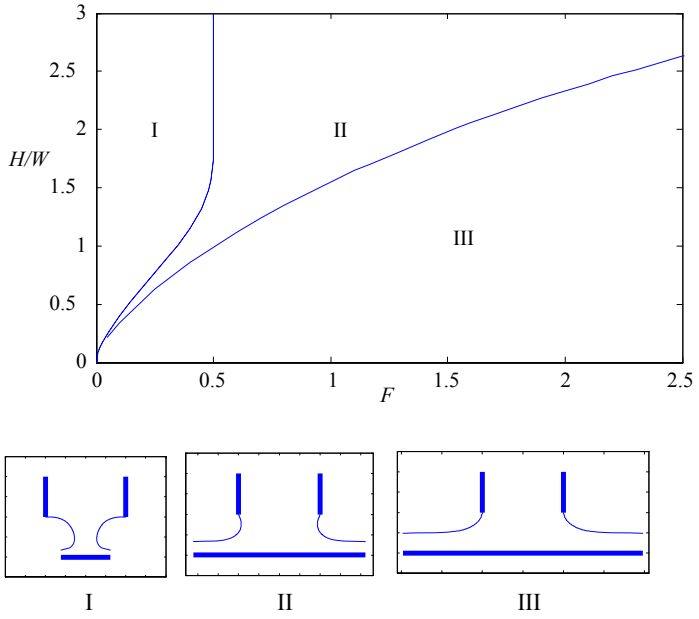

Fig. 1. The incompressible falling jets depend on two parameters, the Froude number F and the aspect ratio between the falling altitude and the pipe width H/W. The two plotted curves divide the (F, H/W) plane into three regions. In region I, the jet emerges from the pipe with a stagnation point. In region II, the jet emerges from the pipe without a stagnation point but experiences squeezing before being deflected by the horizontal plate. In region III, the jet emerges from the pipe without a stagnation point and is immediately deflected.

FORMULATION OF THE INCOMPRESSIBLE PROBLEM

We consider the steady irrotational flow of an incompressible inviscid liquid falling from a pipe of width $2W$ under gravity, hitting a horizontal plate of infinite length placed at a vertical distance H from the bottom edges of the pipe and splitting symmetrically into two jets one on each side of the pipe. As shown in Fig. 2, the stream coming from far inside the pipe (points J, J') hits the horizontal plate, centered at point C, and forms two jets – one on each side – detaching at points A, A' and forming free surfaces $A \to I$, $A' \to I'$.

Due to symmetry, the formulation of the problem is based on the 'right' half of the flow. The results presented in the sequel are simply obtained by superposition of the 'left' and 'right' flows. The point A is taken as the origin of the coordinate system (x, y), x being horizontal and y vertical. The mass flux emerging from the 'right' nozzle is $Q = UW$.

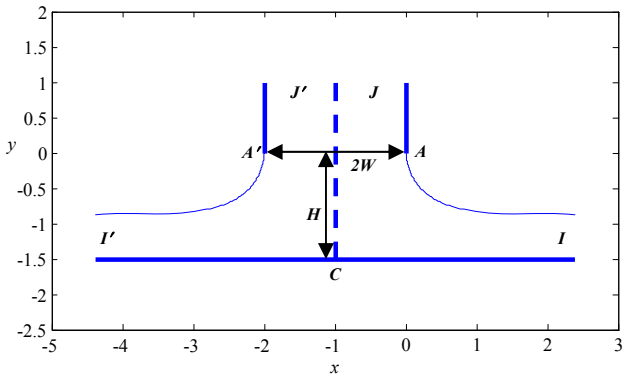

Fig. 2. Sketch of the flow and of the coordinates. The free-surface profile is a computed solution for $H = 1.5$ and $F = 1.5$. Special points are labeled on the boundary.

As the system is governed by the assumptions of irrotationality and incompressibility, we have $(u_x, u_y) = \nabla\varphi$, u_x and u_y being the x- and y-components of the fluid velocity, with Laplace's equation $\nabla^2\varphi = 0$ holding for the velocity potential φ. Bernoulli's equation follows as a first integral of the Euler (momentum) equations of motion. It is valid everywhere inside the fluid and reads

$$\tfrac{1}{2}(u_x^2 + u_y^2) + gy + \frac{p}{\rho} = \text{constant}, \tag{3}$$

where p is the pressure and ρ the liquid density. Assuming a zero pressure on all free surfaces (the flow in the gas is neglected), and taking W and U as the unit length and unit velocity respectively and consequently Q becoming unity, Bernoulli's equation on the free surfaces becomes, in dimensionless form,

$$\tfrac{1}{2}(u_x^2 + u_y^2) + \frac{1}{F^2}\,y = \tfrac{1}{2}u_A^2, \tag{4}$$

where the same symbols are kept for the dimensionless variables for the sake of simplicity. The constant on the right-hand side has been evaluated at point A, where the velocity is purely vertical and $y = 0$. The 2D problem under consideration is solved with the use of conformal mappings. Hence, we define the complex variable $z = x + iy$, the complex potential $f = \varphi + i\psi$ for the velocity potential $\varphi(x, y)$ and the streamfunction $\psi(x, y)$, and the hodograph variable

$$\zeta(z) \equiv \frac{df}{dz} = u_x - iu_y. \tag{5}$$

The flow domain in the plane of the complex potential lies within an infinite strip of height 1. It is then transformed into the upper half of the unit disk in the complex t-plane, with the free surface going onto the upper half of the unit circle and the solid boundaries going onto the real diameter $t \in [-1, 1]$. It is an elementary exercise to show that the transformation from the f-plane to the t-plane can be written in differential form as

$$\frac{df}{dt} = \frac{1}{\pi}\frac{1+t}{t(1-t)} \tag{6}$$

or, in integrated form, as

$$f = \frac{1}{\pi}\ln\left(\frac{t}{(1-t)^2}\right). \tag{7}$$

It is clear that t can be obtained as a function of f explicitly by inverting relation (7). We denote by t_C the image of point C in the t-plane.

The problem now reduces to finding the hodograph variable ζ as an analytic function of t, satisfying Bernoulli's Eq. (4) on the free surfaces and the kinematic boundary condition on the solid boundaries, that is on the real diameter $t\in[-1, 1]$. Christodoulides and Dias (2010) showed that ζ can be sought in the form

$$\zeta(t) = \frac{(t-t_C)^{1/2}}{(t_C)^{1/2}} e^{\Omega(t)}, \tag{8}$$

where the function $\Omega(t)$ is analytic for $|t|<1$, continuous for $|t| \le 1$, and can be expanded in a power series of the form

$$\Omega(t) = \sum_{n=1}^{\infty} a_n t^n. \tag{9}$$

The numerical method used to determine the coefficients a_n is described below.

FORMULATION OF THE COMPRESSIBLE PROBLEM

We consider the same flow, but of a slightly compressible inviscid liquid falling under gravity from a pipe of width $2W$ in the presence of a compressible inviscid gas of much lower density. The two fluids are taken to be immiscible at their interface. The bottom edge of the pipe is at a height H above a horizontal plate and the liquid has an initial vertical velocity U at this edge. Due to the symmetrical nature of this problem, we consider only the 'right' half of the flow.

We use the 2D compressible Euler equations to compute the flow of each fluid away from the interface. These can be formulated as

$$\partial_t V + \nabla\cdot F(V) = S, \tag{10}$$

where

$$V = \begin{pmatrix} \rho \\ \rho u_x \\ \rho u_y \\ \rho(e+\frac{1}{2}|u|^2) \end{pmatrix}, \tag{11}$$

$$F(V) = \begin{pmatrix} \rho u_x & \rho u_y \\ \rho {u_x}^2 + p & \rho u_x u_y \\ \rho u_x u_y & \rho {u_y}^2 + p \\ (\rho e + \frac{1}{2}\rho|u|^2 + p)u_x & (\rho e + \frac{1}{2}\rho|u|^2 + p)u_y \end{pmatrix}, \tag{12}$$

$$S = (0, 0, -g, 0)^T, \tag{13}$$

and where

$$\nabla\cdot F(V) = \partial_x F^1(V) + \partial_y F^2(V). \tag{14}$$

As opposed to the incompressible case, there is an energy equation, in which e denotes the internal energy. To close this system, we also need an equation of state for each fluid. We use the stiffened gas equation, which is a generalization of the ideal gas law:

$$p + \pi_{mat} = (\gamma_{mat} - 1)\rho e, \tag{15}$$

with empirically determined fluid constants π_{liq} = 159290725 Pa, γ_{liq} = 7.0, π_{gas} = 0.0 Pa, and γ_{gas} = 1.16. The speed of sound is given by

$$c = \sqrt{\frac{\gamma_{mat} p + \pi_{mat}}{\rho}}. \tag{16}$$

With the chosen constants for the liquid and with ρ = 1000 kg/m^3, one finds that the speed of sound in the liquid is equal to 400 m/s at atmospheric pressure p = 101325 Pa. Of particular importance is the projection of the flux F with a unit vector n:

$$F(V)\cdot n = (u\cdot n)V + pN, \tag{17}$$

where $N = (0, n_x, n_y, u\cdot n)^T$.

At the interface between the two fluids, it is convenient to consider the problem in Lagrangian coordinates. The compressible Euler equations in 1D can formulated in Lagrangian coordinates as:

$$\partial_t \begin{pmatrix} \tau \\ u \\ e+\frac{1}{2}u^2 \end{pmatrix} + \partial_x \begin{pmatrix} -u \\ p \\ pu \end{pmatrix} = 0 \tag{18}$$

where τ denotes $1/\rho$. The fundamental thermodynamic equation $Tds = de + pd\tau$ yields

$$\begin{aligned} T\partial_t s &= \partial_t e + p\partial_t \tau \\ &= -\partial_t(\tfrac{1}{2}u^2) - \partial_x(pu) + p\partial_x u \\ &= -u\partial_t u - u\partial_x p \\ &= 0 \end{aligned} \tag{19}$$

The change of variables

$$\phi: \begin{pmatrix} \tau \\ u \\ s \end{pmatrix} \to \begin{pmatrix} \tau \\ u \\ e+\frac{1}{2}u^2 \end{pmatrix} \tag{20}$$

transforms (18) into

$$\begin{cases} \dfrac{\partial\tau}{\partial t} - \dfrac{\partial u}{\partial x} = 0 \\ \dfrac{\partial u}{\partial t} + \dfrac{\partial p}{\partial x} = 0 \\ \dfrac{\partial s}{\partial t} = 0 \end{cases}. \tag{21}$$

The Jacobian matrix for this system is given by

$$A(V)=\begin{pmatrix} 0 & -1 & 0 \\ -\rho^2 c^2 & 0 & p_s \\ 0 & 0 & 0 \end{pmatrix}, \tag{22}$$

with eigenvalues

$$\lambda_{-1}=-\rho c \quad < \quad \lambda_0=0 \quad < \quad \lambda_1=\rho c\,, \tag{23}$$

right eigenvectors

$$r_{-1}=\begin{pmatrix} \rho^{-1} \\ c \\ 0 \end{pmatrix}, r_0=\begin{pmatrix} p_s \\ 0 \\ \rho^2 c^2 \end{pmatrix}, r_1=\begin{pmatrix} \rho^{-1} \\ -c \\ 0 \end{pmatrix} \tag{24}$$

and left eigenvectors

$$l_{-1}=\begin{pmatrix} \rho c \\ 1 \\ p_s(\rho c)^{-1} \end{pmatrix}, l_0=\begin{pmatrix} 0 \\ 0 \\ (\rho c)^{-2} \end{pmatrix}, l_1=\begin{pmatrix} \rho c \\ -1 \\ p_s(\rho c)^{-1} \end{pmatrix}. \tag{25}$$

It is easy to verify that the flux term satisfies the equation

$$\partial_t F(V)+A(V)\partial_x F(V)=0\,. \tag{26}$$

Consider an interface which separates two states V^- and V^+. Linearizing yields

$$\begin{aligned} &(E^-): \quad \partial_t F(V)+A(V^-)\partial_x F(V)=0 \\ &(E^+): \quad \partial_t F(V)+A(V^+)\partial_x F(V)=0. \end{aligned} \tag{27}$$

For (E^-), the Riemann invariant associated with the eigenvalue $\rho^- c^-$ is given by

$$\pi^- = l_1^- \cdot F(V)=\begin{pmatrix} \rho^- c^- \\ -1 \\ p_s(\rho^- c^-)^{-1} \end{pmatrix} \cdot \begin{pmatrix} -u \\ p \\ 0 \end{pmatrix} = -p-\rho^- c^- u; \tag{28}$$

for (E^+), the Riemann invariant associated with the eigenvalue $-\rho^+ c^+$ is given by

$$\pi^+ = l_{-1}^+ \cdot F(V)=\begin{pmatrix} \rho^+ c^+ \\ 1 \\ p_s(\rho^+ c^+)^{-1} \end{pmatrix} \cdot \begin{pmatrix} -u \\ p \\ 0 \end{pmatrix} = p-\rho^+ c^+ u. \tag{29}$$

Using an upwind discretization method one can write

$$\pi^-(V^-)=\pi^-(V_{\text{int}}) \quad \text{and} \quad \pi^+(V^+)=\pi^+(V_{\text{int}})\,, \tag{30}$$

which leads to the relation

$$\begin{cases} p_{\text{int}}=\dfrac{\rho^+ c^+ p^- + \rho^- c^- p^+}{\rho^- c^- + \rho^+ c^+}+\rho^- c^- \rho^+ c^+ \dfrac{u^- - u^+}{\rho^- c^- + \rho^+ c^+}\,, \\ u_{\text{int}}=\dfrac{\rho^+ c^+ p^+ + \rho^- c^- p^-}{\rho^- c^- + \rho^+ c^+}+\dfrac{p^- + p^+}{\rho^- c^- + \rho^+ c^+} \end{cases} \tag{31}$$

which was first derived by Braeunig (2007).

NUMERICAL METHOD FOR THE INCOMPRESSIBLE PROBLEM

The coefficients a_n in the power series (9) are real and are determined by using a collocation Galerkin method. The infinite series is truncated. Given the distance $H \in (0, \infty)$, the discretized system is solved by Newton's method for given values of the Froude number $F \in (0, \infty)$, thus giving a two-parameter family of solutions. See Christodoulides and Dias (2010) for details.

NUMERICAL METHOD FOR THE COMPRESSIBLE PROBLEM

We use the direct Eulerian finite volume solver VFFC-IC (*Characteristic Fluxes Finite Volume with Interface Capturing*), developed by Braeunig, Desjardins and Ghidaglia (2009), to solve this system. We impose a finite computational domain, discretized into an evenly subdivided rectangular grid. At each volume element cell we store a volume fraction $0 \le \alpha \le 1$ and the conservative variables for each material, V_1 and V_2. We use time-splitting and alternating horizontal and vertical traversals for each time step.

For a cell with $0 < \alpha < 1$ we create at each time step an artificial interface between the two materials based on the volume fraction of the cell and of the eight neighboring cells. Wherever we have such an interface, we use (33) and the method described below.

To determine the evolution of a volume element $\Omega(t)$ with boundaries of potentially nonzero velocity

$$\partial\Omega(t)=\Gamma(t)=\Gamma_{u=0}\cup\Gamma_{u\neq 0}\,, \tag{32}$$

we can derive the following result:

$$\frac{\left|\Omega^{n+1}\right|V^{n+1}-\left|\Omega^{n}\right|V^{n}}{\Delta t}+A(\phi_{u_{\text{int}}=0}+p_{\text{int}}N(u_{\text{int}},p_{\text{int}}))=0\,. \tag{33}$$

We calculate the numerical flux terms Φ from the physical fluxes $F(V)$ based on an *upwind* strategy. At a face Γ with normal $\boldsymbol{n}$, we have

$$\phi(\Gamma,n)=\left(\frac{F(V_l)+F(V_r)}{2}-sign\left(J\left(V_\Gamma,n\right)\right)\frac{F(V_r)-F(V_l)}{2}\right)\cdot n, \tag{34}$$

where

$$sign(J)=R\left(V,n\right)diag\left(sign\left(\lambda\left(V,n\right)\right)\right)\left(V,n\right), \tag{35}$$

with $J(\boldsymbol{V,n})$ being the Jacobian of $F(\boldsymbol{V,n})$ and with $R(\boldsymbol{V,n})$, $L(\boldsymbol{V,n})$, and $\lambda(\boldsymbol{V,n})$ being the matrices of right and left eigenvectors and the set of eigenvalues of $J(\boldsymbol{V,n})$.

A description of the boundary conditions can be found in Ghidaglia and

Pascal (2005). We impose wall conditions on the left and bottom edges of the computational domain, an entry condition at the location of the pipe, and Neumann-like boundary conditions elsewhere. Let Φ_K denote the flux at a boundary element K. At a wall condition we have $u \cdot n = 0$, so

$$\phi_K = (0, pn_x, pn_y, 0)^T . \tag{36}$$

For boundary elements where $u \cdot n \neq 0$, we need external information. It can be shown that the eigenvalues of the Jacobian $J(V_\Gamma, n)$ are given by

$$\begin{aligned} \lambda_1(V_\Gamma, n) &= (u \cdot n) - c, \\ \lambda_2(V_\Gamma, n) &= (u \cdot n), \\ \lambda_3(V_\Gamma, n) &= (u \cdot n), \\ \lambda_4(V_\Gamma, n) &= (u \cdot n) + c. \end{aligned} \tag{37}$$

Let V_K be a volume element adjacent to the boundary. In the case of a supersonic outlet $\boldsymbol{u} \cdot \boldsymbol{n} > c$, all eigenvalues are positive and thus from (35) we need only information from V_K:

$$\phi_K = F(V_K, n) . \tag{38}$$

For a supersonic inlet $\boldsymbol{u} \cdot \boldsymbol{n} < -c$, we must impose all information about the flux:

$$\phi_K = F(V_{out}, n) . \tag{39}$$

For a subsonic outlet $0 < \boldsymbol{u} \cdot \boldsymbol{n} < c$, we must impose one external condition; here we impose the external pressure $p_{out} = p_{atm}$ and calculate the remaining terms to satisfy the condition

$$l_i \cdot F(V_K, V) = l_i \cdot \phi_K , \quad i = 1, 2, 3. \tag{40}$$

For a subsonic inlet $-c < \boldsymbol{u} \cdot \boldsymbol{n} < 0$, we must impose three conditions. At the entry condition at the pipe, we impose $\rho_{out} = 1000$ kg/m^3 and $\boldsymbol{u}_{out} = \boldsymbol{U}$. For the Neumann-like conditions we have $\rho_{out} = \rho_{in}$, $\boldsymbol{u}_{out} = \alpha \cdot \boldsymbol{u}_{in}$, and $p_{out} = p_{atm}$. We then calculate the remaining condition to satisfy

$$l_4 \cdot F(V_K, V) = l_4 \cdot \phi_K . \tag{41}$$

The time step dt is obtained from the CFL stability condition:

$$dt < \min_i \left(\frac{Vol_i}{A_\Gamma \max_k \left| (\lambda_i)_k \right|} \right), \tag{42}$$

where A_Γ is the area of face Γ.

RESULTS

For the compressible calculations, the gas density with a background pressure $p = 101325$ Pa is equal to 4 kg/m^3 while the liquid density is equal to 1000 kg/m^3. The density ratio is therefore equal to 0.004, which is a typical value for the NG/LNG mixture. In Fig. 2, we have already shown a computed solution (incompressible flow) with $H = 1.5$ (i.e. the H/W ratio is 1.5) for a relatively large value of the Froude number $F = 1.5$. One can see that the flow leaves the pipe at A (A') tangentially at an angle of 180^o and gradually moves to the right (left) forming a single-free-surface jet that moves along the horizontal plate to $+\infty$ ($-\infty$). Keeping F fixed at 1.5 and letting H vary has the following effect in the behavior of flow. As shown in Fig. 3 for 'small' $H = 0.2$ the flow, after detaching, moves to the right (left) almost immediately and continues along the horizontal plate to $+\infty$ ($-\infty$). Fig. 3 also shows a compressible flow with the same H and F but with a Mach number $M = 0.01175$. For 'large' $H = 3.0$ (see Fig. 4) the jet becomes thinner (i.e. the fluid is like being *squeezed*) after detaching, then is gradually diverted and finally moves along the horizontal plate to $+\infty$ ($-\infty$). Again a compressible flow with $M = 0.01175$ is also shown.

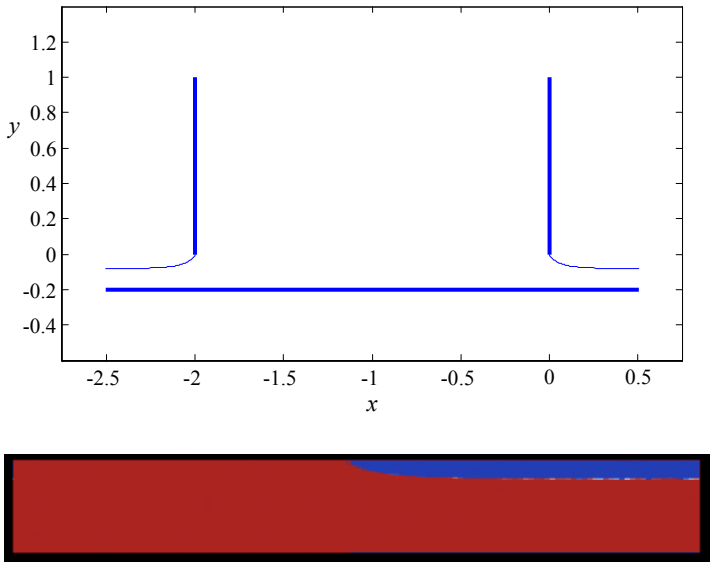

Fig. 3. Free-surface profiles for $H = 0.2$ and $F = 1.5$. Top: Incompressible flow; Bottom: Compressible flow with $M = 0.01175$.

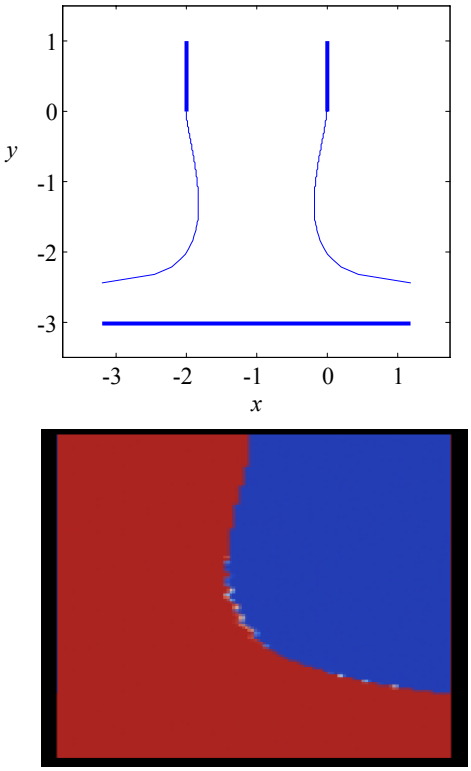

Fig. 4. Free-surface profiles for H = 3.0 and F = 1.5. Top: Incompressible flow; Bottom: Compressible flow with M = 0.01175.

Increasing the Froude number to 'large' values has no effect on the behavior of the flow for small to medium heights H. This behavior though, persists even for large values of H, as demonstrated in Fig. 5, where F = 10 and H = 3.0. One can observe that there is no squeezing of the free surfaces. In fact, for H = 3.0, the *transition* value of F (separating the regions with and without squeezing) is 3.3.

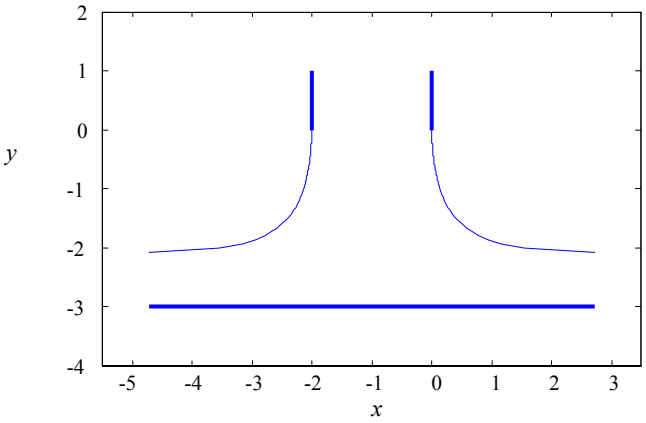

Fig. 5. Free-surface profiles for parameter values H = 3.0 and F = 10. The result is for an incompressible flow.

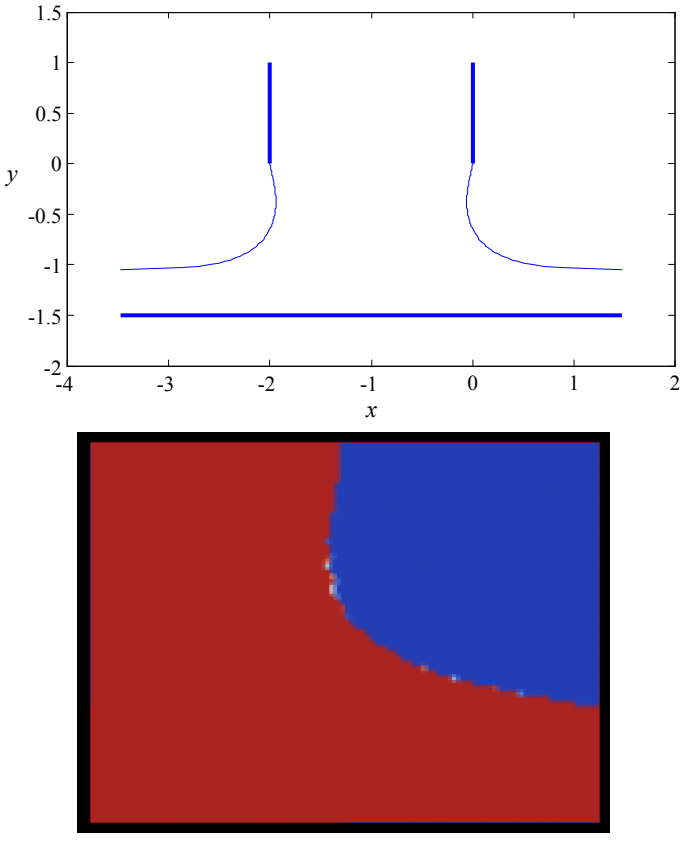

Fig. 6. Free-surface profiles for H = 1.5 and F = 0.7. Top: Incompressible flow; Bottom: Compressible flow with M = 0.0054775.

The curve along which the transition between squeezing and no-squeezing occurs is shown in Fig. 1. It is the curve that separates region II from region III. Because of the shape of that boundary, it is clear that decreasing the Froude number leads to more and more values of the height H with the occurrence of the squeezing of the free surfaces. An example is shown in Fig. 6, where F = 0.7 and H = 1.5. In fact, for H = 1.5, the transition value of F (separating the regions with and without squeezing) is 0.93. A compressible flow with M = 0.0054775 is also shown.

To summarize, we have so far found two types of flows: flows without squeezing in region III (these flows look relatively similar to the equivalent flow in the absence of gravity) and flows with squeezing in region II (these flows are strongly influenced by gravity). The incompressible and compressible flows look qualitatively similar.

FLOWS WITH A STAGNATION POINT AND OTHER FLOWS

The only possible values for the angles between the vertical side of the pipe and the free surface are 90° and 120°. The 90° case corresponds to the free surface leaving the side of the pipe horizontally, while the 120° case corresponds to the free surface leaving the side of the pipe at a 60° angle from the vertical. The singularities in the expression for the hodograph variable ζ of must be modified. It turns out that such flows exist only for 'small' Froude numbers, $F \le 0.50 = F_C$. Actually, this critical value F_C corresponds exactly to the one found by Vanden-Broeck (1984) in his study of jets falling from a nozzle. Even though the critical value F_C is very close to 1/2, there is no obvious reason why it should be exactly 1/2.

The curve that gives the boundary between regions I and II is given in Fig. 1. As H increases, F approaches the limiting value of 0.5, which corresponds to the configuration in the absence of the horizontal plate. A typical flow is shown in Fig. 7 for H = 1.01, corresponding to a Froude number of F = 0.35. One can see that the flow detaches at A (A') at an angle of 120° and gradually turns to the right (left) and moves along the horizontal plate to $+\infty$ ($-\infty$). A compressible flow with M = 0.00274 is also shown.

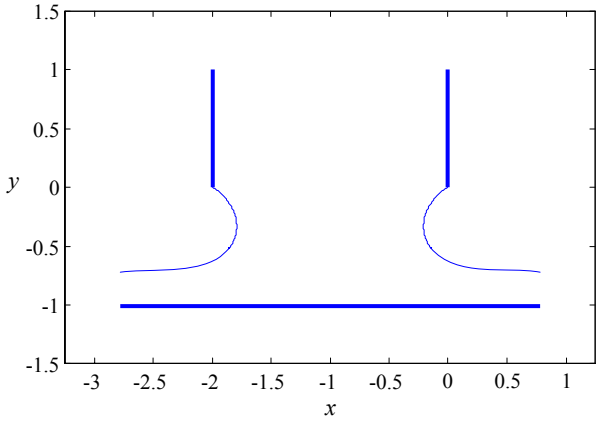

Fig. 7. Free-surface profiles with 120° stagnation points at A, A' for H = 1.01. The Froude number F = 0.35 comes as part of the solution. Top: Incompressible flow; Bottom: Compressible flow with M = 0.00274.

For the 90° stagnation points the numerical process is exactly identical to the previous one, where the coefficients a_n in the power series (10) are real and can be determined by a collocation Galerkin method, giving again a two-parameter family of solutions. It turns out that such flows exist for 'small' Froude numbers ($F < F_C$, see the 120° case) for values of H larger than the value of H corresponding to the 120° case. For instance, for F = 0.35 such solutions exist for 1.01 ≤ H, where 1.01 is the corresponding H for the 120° case. An example of a flow with 90° stagnation points is demonstrated in Fig. 8 for H = 0.5 and F = 0.1. Such solutions fall into region I of Fig. 1 above. A compressible flow with M = 0.0007825 is also shown.

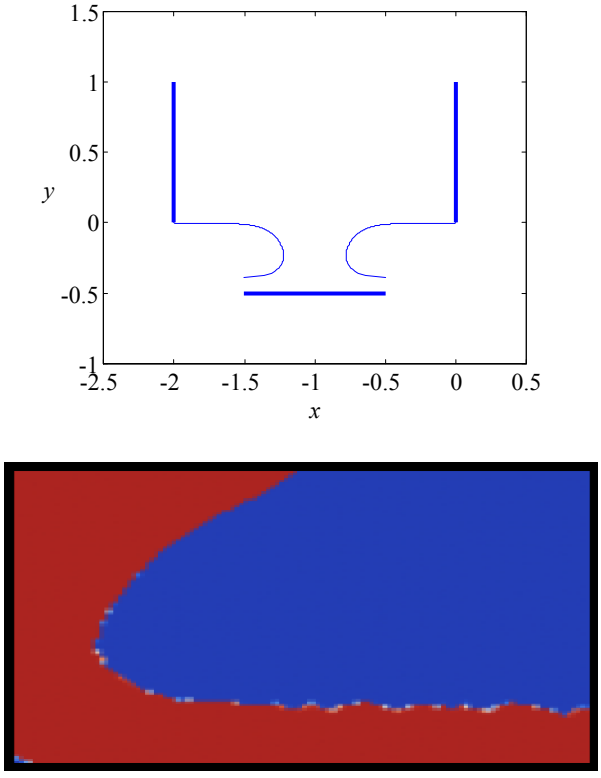

Fig. 8. Free-surface profiles with 90° stagnation points at A, A' for H = 0.5 and F = 0.1. Top: Incompressible flow; Bottom: Compressible flow with M = 0.0007825.

PRESSURE ALONG THE PLATE

The results in this section are only for the incompressible flows. It is expected to have results for the compressible flows at the conference.

Along the horizontal plate, the dimensionless Bernoulli's equation simply reads

$$|\zeta|^2 - \frac{2}{F^2}H + p = |\zeta_A|^2, \tag{43}$$

where the pressure p has been non-dimensionalized by $\rho U^2/2$ and $|\zeta_A|$ is the magnitude of the velocity at point A. Fig. 9 shows a typical pressure profile along the plate for H = 1.5 and F = 1.5 (see case of Fig. 2).

At the centre of the plate (point C) the pressure is maximum since the velocity is 0. In the case where A is a stagnation point, $|\zeta_A|$ becomes identically 0. For a given Froude number F, one can obtain the maximum pressure as a function of height H. In Fig. 10 are presented corresponding results for F = 0.7, 1.5 and 5.0. One clearly can observe that the curves exhibit a minimum. This minimum can be explained as follows. For small values of H, the flow has little space between the edge of the pipe and the horizontal plate, as in Fig. 3. The flow is not affected much by gravity and is close to the no-gravity case considered in the monograph by Milne-Thomson (1996, Example XII.10 and Fig. 14.8*b*), where an analytical solution was provided. Using our notation, the relationship between H (which is in fact H/W) and the ultimate width $d = D/W$ of the jet in contact with the plate (D being the far-field depth of the stream of fluid on the horizontal plate) reads

$$H = d + \frac{1+d^2}{\pi}\ln\left(\frac{1+d}{1-d}\right). \tag{44}$$

In the limit of small H, one finds a constant ratio H/d equal to $1 + 2/\pi$. Let v denote the dimensionless velocity of the uniform flow along the plate (in the far field). Since the mass flux is equal to 1, $d = 1/v$. Neglecting gravity, it follows that $|\zeta_A| = v$. At the centre of the plate (point C), Bernoulli's equation yields approximately

$$p_C \approx |\zeta_A|^2 = \frac{1}{d^2} = \frac{(1+2/\pi)^2}{H^2}. \tag{45}$$

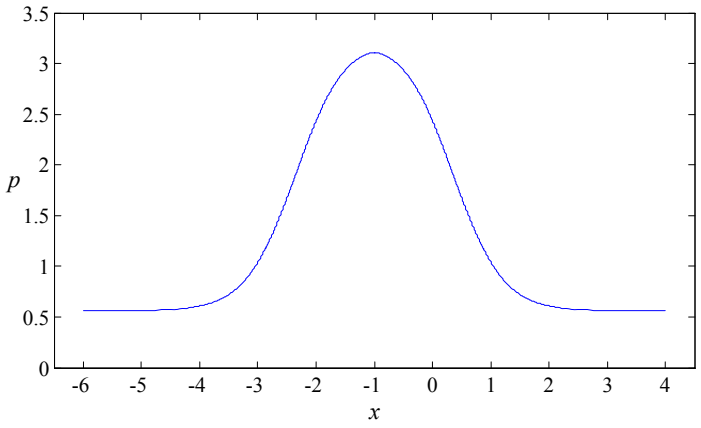

Fig. 9. Pressure profile along the plate for H = 1.5 and F = 1.5.

The pressure increases quite rapidly as H decreases, as can be seen in Fig. 10. The behavior near the minimum is due to the 'squeezing' of the free surfaces already discussed above. The two free surfaces tend to 'squeeze' the internal middle flow, thus affecting the pressure exerted at C, which increases despite the increase of the distance H. This phenomenon becomes weaker for higher values of the Froude numbers.

Or rather, the minimum occurs at higher values of H. Again an asymptotic analysis allows us to obtain an estimate for the pressure for large values of H. In that case, the jet experiences a long free fall before hitting the plate. The term containing H in Bernoulli's Eq. (43) is now much larger than the term containing $|\zeta_A|$ so that

$$p_C \approx 2\frac{H}{F^2}. \tag{46}$$

The pressure increases linearly as H increases. For large values of the Froude number, the slope $2/F^2$ is quite small, as can be seen in Fig. 10(c).

Let us finally provide a few results with physical dimensions. Taking U = 2 m/s, H = 15 m, W = 4 m and ρ = 1000 kg/m^3 (with g = 9.81 m/s^2) yields F = 0.32 and, using Eq. (46),

$$p_C - p_{atm} = 73.575\left(\frac{1}{2}\rho U^2\right) = 1.475 \text{ bar}, \tag{47}$$

which is a relatively large value. Taking now U = 2 m/s, H = 1 m, W = 4 m and ρ = 1000 kg/m^3 yields again F = 0.32 and, using (45),

$$p_C - p_{atm} = 42.856\left(\frac{1}{2}\rho U^2\right) = 0.857 \text{ bar}, \tag{48}$$

which is still a relatively large value. For this particular value of the Froude number (F = 0.32), the minimum for the dimensionless pressure at point C is 17.008. For U = 2 m/s, W = 4 m and ρ = 1000 kg/m^3, it turns out that at the minimum $p_C - p_{\text{atm}}$ = 0.340 bar.

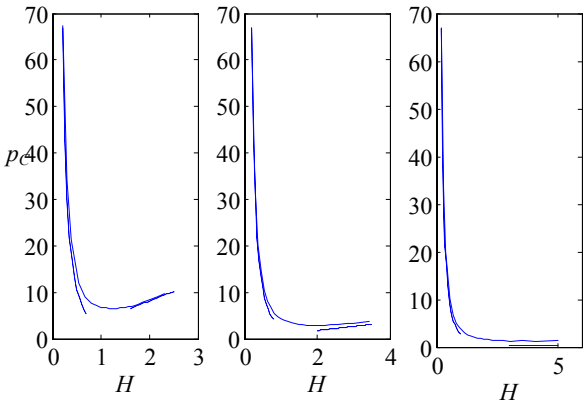

(a) (b) (c)

Fig. 10. Values of the maximum pressure, at the centre C of the plate, as a function of H for (a) F = 0.7, (b) F = 1.5, (c) F = 5.0 (solid lines). The dashed and dotted lines represent respectively the approximation for *small* and *large* values of H.

DISCUSSION

We have seen a good qualitative agreement between the compressible and incompressible flows. However this is preliminary work and more results will be presented at ISOPE 2010.

This research has been supported by ANR HEXECO, Project n^o BLAN07-1_192661 and by the 2008 Framework Program for Research, Technological development and Innovation of the Cyprus Research Promotion Foundation under the Project ΑΣΤΙ/0308(BE)/05.

The authors thank Farshad Navah, who initiated the part of the study dealing with compressible flows during a training at Ecole Normale Supérieure de Cachan in the spring of 2009.

REFERENCES

Braeunig, J-P (2007). Sur la simulation d'écoulements multi-matériaux par une méthode eulérienne directe avec capture d'interfaces en dimensions 1, 2 et 3, Thèse de Doctorat No 2007/85, Ecole Normale Supérieure de Cachan.

Braeunig, J-P, Brosset, L, Dias, F and Ghidaglia, J-M (2009). "Phenomenological study of liquid impacts through 2D compressible two-fluid numerical simulations," *Proceedings of the Nineteenth International Offshore and Polar Engineering Conference, Osaka, Japan, 21–28*.

Braeunig, J-P, Brosset, L, Dias, F, Ghidaglia, J-M and Maillard, S (2010). "On the scaling problem for impact pressure caused by sloshing," in preparation.

Braeunig, J-P, Desjardins, B, Ghidaglia, J-M (2009). "A totally Eulerian finite volume solver for multi-material fluid flow." *European Journal of Mechanics B/Fluids*, 28, pp 475-485.

Christodoulides, P and Dias, F (2009). "Impact of a rising stream on a horizontal plate of finite extent," *J. Fluid Mech.*, 621, pp 243–258.

Christodoulides, P and Dias, F (2010). "Impact of a falling jet," *J. Fluid Mech.*, accepted.

Ghidaglia, J-M and Pascal F (2005). "The normal flux method at the boundary for multidimensional finite volume approximations in CFD", *European Journal of Mechanics B/Fluids*, 24, pp 1–17.

Milne-Thompson, LM (1996). "*Theoretical Hydrodynamics*," Fifth Edition, Dover Publications, New-York, 743pp.

Vanden-Broeck, J-M (1984). "Bubbles rising in a tube and jets falling from a nozzle", *Phys. Fluids*, 27(5), pp 1090–1093.